Balloon measurements of the vertical ionization profile over southern Israel and comparison to mid-latitude observations

Article

Accepted Version

Published version at: http://www.sciencedirect.com/science/article/pii/S1364682616303029
To link to this article DOI: http://dx.doi.org/10.1016/j.jastp.2016.10.003

Publisher: Elsevier

Balloon measurements of the vertical ionization profile over southern Israel and comparison to mid-latitude observations

Roy Yaniv[1], Yoav Yair[2], Colin Price[1], Keri Nicol[3], Giles Harrison[3], Anton Artamonov[4] and Ilya Usoskin[4]

[1] Department of Geosciences, Tel-Aviv University, Tel-Aviv, Israel.
[2] School of Sustainability, Interdisciplinary Center (IDC) Herzliya, Israel
[3] Department of Meteorology, University of Reading, United Kingdom.
[4] Space Climate group, Faculty of Science, University of Oulu, Finland.

Abstract

Airborne measurements using meteorological balloons were conducted for the first time from southern Israel (geographic 30°35’N, 34°45’E geomagnetic 27°6’N 112°23’E) for measuring the vertical ionization profile during solar cycle 24. The results show the differences (increase of ~30%) in count rates as we proceed from solar maximum toward solar minimum. The observed altitude of maximum ionization (the Regener-Pfotzer maximum) was between 17-20 km, and it agrees well with results from other simultaneous measurements conducted at different latitudes (Reading, UK and Zaragoza-Barcelona, Spain). When compared with predictions of an analytical model, we find a highly significant correlation (R^2=0.97) between our observations and the computed ionization profiles. The difference in count rates can be attributed to the height of the tropopause due to the model using a US standard atmosphere that differs from the measured atmospheric parameters above Israel.

1. Introduction

Over land and within the boundary layer (few hundred meters) the atmosphere is mostly ionized by radiation emitted from the decay of radioactive isotopes in the Earth's crust. Hess [1912] studied the ionization profile in the atmosphere and postulated that ionization should therefore decrease with altitude since the radioactive elements have a source near the surface. However, using balloon measurements Hess found that ionization increased at altitudes above 10 km, and interpreted the results as caused by an external source, namely galactic cosmic rays (GCR). He claimed that the penetration depth of these particles was dependent on the energy spectrum of the incoming radiation [Hess 1912]. Regener extended Hess' measurements using balloons, reaching heights up to 20km (Regener 1933). They found that the ionization from cosmic rays reaches its maximum value at altitudes between 17-24 km and is known as the Regener-Pfotzer maximum (RP max) and is geomagnetic-latitude dependent (Pfotzer 1936, Carlson and Watson 2014). Figure 1 shows past and present measurements of the ionization profile (counts/sec/cm^2/steradian) from a V-2 rocket up to 80 km at 40° geomagnetic latitude, and a sounding balloon launch up to 30km from Reading, UK with a ionization model fit overlaid. In both locations the RP max can be clearly observed [Israël 1970; Harrison et al., 2014].

Up to 40 km above the surface the main ionization source in the atmosphere is GCR and, sporadically in the polar region, solar protons [Mironova et al., 2015]. Balloon measurements of charged particle fluxes (> 1MeV) and ion production rates have been performed continuously from 1957 by the Lebedev Physics Institute, Russia [Bazilevskaya et al 2000, Bazilevskaya et al 2008]. They found a correlation between the ratio of ion production rate (q) and the cosmic charged particle flux (J) during days with no solar activity at polar latitudes given by: $\frac{q}{J} = Ae^{-BH}$ (where A= 119.86 cm−1 ; B = 0.148, and H is the altitude [km] – Bazilevskaya et al 2000 their Figure 4). The flux of cosmic rays reaching the atmosphere at any given location is a function of the energy spectrum, which is also impacted by solar activity, on short and long temporal scales and by the geomagnetic rigidity cutoff, effectively determined by the geomagnetic latitude. The rigidity is a key parameter for particle motion in magnetic fields and is defined as the particle's momentum over charge: particles cannot penetrate to locations where the geomagnetic cutoff is greater than the particle's rigidity (Bazilevskaya 2005, Smart et al 2006, Mironova et al., 2015).

Simultaneous ground and airborne measurements using a balloon equipped with an ionization counter (based on a Geiger tube) have previously been performed during quiet atmospheric conditions and during a solar flare event from Reading, UK [Nicoll and Harrison, 2014; Harrison et al., 2014]. During the solar flare, the X-ray burst was followed by a solar proton event that caused changes in the atmospheric electrical properties of the potential gradient and the conduction current at ground level, with an observed increase of more than 20% in the ionization at 20km, deduced from the RP max values that were measured relative to quiet conditions.

2. Methodology

2.1 Instrumentation

Measurements of the atmospheric ionization up to the height of 35 km were conducted using standard radiosonde balloons equipped with additional disposable ionization sensors developed by the University of Reading. The ionization sensor is composed of two LND714 miniature Geiger tubes which uses a microcontroller to count the number of ionization events (the impact of a gamma photon counts as one event) that occur within each tube per minute interval [Harrison et al., 2013]. Count rates reported here are the mean count rate from both tubes. Each Geiger tube was calibrated by the manufacturer using a Co-60 Ionization source with a gamma sensitivity of 1.5 (counts s^{-1})/(mR $hour^{-1}$) (Harrison et al., 2012; Harrison et al., 2013). The ionization sensor is interfaced to a standard Vaisala RS92 radiosonde via the PANDORA data acquisition system (Harrison et al, 2012).

The balloons were launched from the Wise Observatory in Mitzpe Ramon (30^o35'N, 34^o45'E, altitude 850 m a.s.l.). This location is in an arid region of the southern part of Israel (the Negev highland desert) remote from Israel's major cities and other sources of pollution. The area's climate typically exhibits hot and dry summers with average daily temperature of 30 $^{\circ}$C and cold winters with average temperature of 6 $^{\circ}$C. These conditions readily facilitate other atmospheric electrical measurements (vertical E-field, vertical conduction current, ELF and VLF), as described in Price and Melnikov (2004), Elhalel et al. (2014) and Yaniv et al. (2016). We note that these are the first such measurements ever conducted in Israel, and for that matter, in this low geomagnetic latitude range. Thus, the measurements offer a much needed addition to the global map of cosmic ray ionization, which is traditionally based on balloon measurements conducted at mid and high-latitudes.

2.2 Model Description

We used the CRAC:CRII model of atmospheric ionization [Usoskin and Kovaltsov, 2006; Usoskin et al., 2010], based on Monte Carlo calculations which simulate the ionization by cosmic rays (interactions of particles (protons, alpha-particles and heavier species) and locally produced secondary particles (protons, electrons, neutrons and muons)), enabling a comparison between observations and theoretical predictions. The model output provides the vertical profile of the ion production rate and is applicable to a US standard atmosphere. The predictions of the model have been validated over a wide range of geographical latitudes and altitudes [Usoskin and Kovaltsov 2006; Harrison et al 2014]. The model can assess the ionization rate by cosmic rays, by considering the geomagnetic rigidity cutoff at the site and the actual cosmic ray intensity as monitored by ground-based neutron monitors.

Atmospheric ionization is mostly defined by the flux of GCR outside the atmosphere, which is modulated by solar activity: the GCR flux is greater for low solar activity periods and visa versa. Solar modulation of GCR is often quantified via the modulation potential [Usoskin et al., 2005]. Values of the modulation potential for the days of the reported balloon flights are given in Table 1. One can see that the modulation potential decreased in time between the launches, reflecting the declining phase of solar activity in the present solar cycle.

3. Results

Six balloon launches were conducted during the period from October 2014 to June 2016 reaching altitudes of ~18, 29, 28, 34, 35 and 28km. Starting with launch #3 we also used a parachute to measure parameters during descent. Table 1 summarizes the operational aspects of our airborne campaign including flight duration, peak pressure at the highest altitude, lowest temperature measured during the flight and the highest count rate representing the RP max altitude. Figure 2 shows the flight trajectories on a regional map, indicating that some balloons drifted with the stratospheric winds to Jordan and Egypt, and were thus not retrievable.

Figures 3a, 3b and 3c present the vertical profiles of the temperature, pressure and relative humidity respectively showing the meteorological conditions for each launch. Figures 3a and 3b also show temperature and pressure from the U.S. Standard

Atmosphere 1976, (NASA-TM-X-74335), which agree well with the sounding profiles, although some differences can be clearly noted, as we will discuss later on.

Figure 4a shows the count rates of the Geiger counters as a function of altitude for each launch and the mean calculated ionization curve (black line) which peaks in the height range of 17-20 km. According to the 1976 US standard atmosphere values (http://www.digitaldutch.com/atmoscalc/), the height range of 17-20 km measured in the mean ionization curve corresponds to the pressure of 100 mbar as shown in Fig. 4b. Figure 4b is a fit of the count rate versus the measured atmospheric pressure and is in agreement with Fig. 1b. Figure 4b shows that from 2014 to 2016 the ionization value had steadily increased by ~30%.

Bazilevskaya (2014) noted an impact of the solar cycle on the flux of GCR arriving to Earth's atmosphere. Maximum solar activity diminishes the flux of GCR while minimum activity increases the flux of GCR. Figure 5 shows the negative linear correlation between the RP max counts per minute and the modulation potential. Flight #4 (27 Aug 2015) was conducted during an M class solar flare event with Kp=7 while flight #5 was conducted in fair weather on a quiet solar day.

The second launch was conducted simultaneously with other launches at various locations in order to compare the vertical ionization profiles at different geomagnetic latitudes during 22nd -24th October 2014 (Makhmutov et al., 2015). Figure 6 shows the fit of the ionization profile as was measured by ionization sensors from Mitzpe Ramon (Israel), Zaragoza-Barcelona (Spain) and Reading (UK). We can clearly see the differences in the RP maximum altitude and the count rate as a function of the geomagnetic latitudes. The Reading flight shows a higher count rate, followed by Zaragoza-Barcelona measurement while the Israeli flight shows the lowest count rate. Figure 7 presents the CRAC:CRII model results of the ion production rate as a function of height for the Israel-Spain-UK balloon flights. We used the model to simulate the ionization rate in the atmosphere as a function of the geomagnetic latitudes for the simultaneous launches conducted from Israel, Spain and the UK during 22-24 Oct 2014. Harrison et al., (2014) used a factor of 2.95 for a standard atmosphere to convert the ionization count rates (in counts min^{-1}) to ion production rates. Using this conversion coefficient we found a good correlations (R^2>0.9) between the actual measurement from Israel and the model from the 22 Oct 2014 (Figure 8 top) and the 14 May 2015 launch (Figure8 bottom).

4. Discussion

We present results of airborne measurement conducted for the first time above Israel and from a low latitude location, adding new information on the latitudinal dependence of cosmic ray induced ionization, and complementing the majority of airborne measurements that were performed at mid and high latitudes over Europe, Russia and the US.

The difference (10-35% lower) in the meteorological parameters shown in figure 3a and 3b compared with the U.S standard atmosphere model is especially pronounced in the temperature profile near the tropopause. As discussed below, this US Standard Atmosphere, when used in the CRAC:CRII model, is the main reason for differences between our observations and the model results. Figure 3c also shows large variability in the vertical profile of the relative humidity, indicating periods when the balloon ascended through layers of visible clouds. We visually observed and identified the relevant cloud types, as indicted in the graphs.

4.1 Solar activity impact on ionization:

The ionization increase shown in Figure 4a and Figure 4b results from the overall increase of the GCR flux impacting the Earth due to a decrease in the activity of the sun – reflecting the declining phase of solar cycle 24. Table 1 shows values of the modulation potential (cosmic ray modulation parameter deduced from the sunspot index (Nymmik et al., 1996). It is clearly evident from Figure 5 that ionization count rates increase from ~30 cpm to ~50 cpm as the modulation potential decreases, as more GCR penetrate into the Earth's atmosphere indicating that the sun is approaching solar minimum. During a solar event that occurred during the launch of 27 Aug 2015 (Kp 7), we observed no impact on the ionization profile, likely because of the high cutoff rigidity at the latitude of Israel.

We can conclude that short term variations are too small to be recorded using our instrument, but long term variations in solar activity can be monitored. Similar results were found by Harrison (2014) during the rising phase of solar cycle 24 toward solar maximum with ionization values of the RP max decreasing from around 80 cpm in 2013 to 60 cpm in 2014.

4.2 Geomagnetic latitude effect on ionization:

The differences found between the ionization values from Israel, Spain and the UK shown in Figure 6 are due to geomagnetic shielding (stronger deflection of charged GCR particles by the magnetosphere at the lower latitude of Israel). While high and mid-latitude measurements of the vertical ionization profile are quite abundant [Nicoll 2012], results in low-latitudes and sub-tropical regions are quite rare, and none have been reported in the geomagnetic latitude of Israel (~27N) where the cutoff rigidity is 10.3GV (compared to Spain 4.6GV and the UK 3.6GV). It is observable that the altitude of the RP max at all locations is in good agreement while the intensity of the GCR penetrating decrease as we proceed from polar to equatorial latitudes – values ranged around 25, 40 and 50 cpm for Israel, Spain and UK respectively. Measurements in polar latitudes (Mirny, Antarctica (geomagnetic latitude 67.23 S) with cutoff rigidity of 0.03 GV and Apatity, Russia (geomagnetic latitude 68.14 N) with cutoff rigidity of 0.56 GV) obtained by Makhmutuv et al (2014) on the same day but with a different instrument found higher ionization values than the UK.

The model results shown in Figure 7 agree well with the simultaneous measurements showing that ion production rates (ion pairs/cm^3/s) are larger at higher latitudes where the cutoff rigidity is smaller and lower at lower latitudes where the cutoff rigidity is greater, thus, confirming the results presented in Figure 6. Model results for other balloon flights were in good agreement as well while the small differences are likely due to the use of the Standard US atmosphere in the model rather than the actual atmospheric density profiles from the balloon measurements.

5. Summary

Balloon measurements of the vertical ionization profile have been conducted for the first time in Israel. We found that the Regener-Pfotzer maximum to be in the expected altitude range of 17-20 km at an atmospheric pressure of ~100 mbar. The effect of the present phase of solar cycle 24 is clearly evident in the measured ionization count rates showing an increase in ionization due to increases in GCR fluxes as expected from the declining phase toward the next solar minimum. Simultaneous measurements from different latitudes using the same Geiger counters found a latitudinal dependence of the count rates as expected – higher count rates (~50 cpm) for the mid-latitudes of Spain and UK where the geomagnetic rigidity is lower compared to the low latitude of Israel (~25 cpm). Model calculations of ion pair-production rate profile were found to correlate positively (R^2>0.9) with the measurements.

Acknowledgments

This research is supported by the Israel Science Foundation (grant No. 423/13).

The work of A.A. and I.U. was done in the framework of ReSoLVE Centre of Excellence (Academy of Finland, project 272157).

The ionization sensor developed under STFC grant ST/K001965/1. KAN acknowledges an early Career fellowship of the Leverhulme Trust (ECF-2011-225) and NERC Independent Research Fellowship (NE/L011514/1).

References:

Bartlett, D.T., Tommasino, L., Beck, P., Wissmann, F., O'Sullivan D., Bottollier-Depois, J.-F. and Lindborg L. Investigation of Radiation Doses at Aircraft Altitudes during a Complete Solar Cycle: DOSMAX- A collaborative Research Program. Presented at the 12th Biennial Topical Meeting at XXX 2002.

Bazilevskaya G.A., Krainev M.B., Makhmutov V.S., Effects of cosmic rays on the earth's environment, J. Atmos. Sol.-Terr. Phys. 62, 1577–1586, 2000.

Bazilevskaya G.A., Solar cosmic rays in the near Earth space and the atmosphere. Adv. Space Res. 35, 458–464, 2005.

Bazilevskaya G.A., Usoskin I.G., Flückiger E.O., Harrison R.G., Desorgher L., Bütikofer R., Krainev M.B., Makhmutov V.S., Stozhkov Y.I., Svirzhevskaya A.K., Svirzhevsky N.S., Kovaltsov G.A., Cosmic ray induced ion production in the atmosphere. Space Sci. Rev. 137, 149–173, 2008.

Bazilevskaya, G. A., Cliver, E. W., Kovaltsov, G. A., Ling, A. G., Shea, M. A., Smart, D. F., & Usoskin, I. G., Solar cycle in the heliosphere and cosmic rays. Space Science Reviews, 186(1-4), 409-435, 2014.

Carlson, P., & Watson, A. A. (2014). Erich Regener and the ionization maximum of the atmosphere. History of Geo-and Space Sciences, 5(2), 175.

Elhalel G., Yair Y., Nicoll K., Price C., Reuveni Y., and Harrison R. G., Influence of short-term solar disturbances on the fair weather conduction current, J. Space Weather Space Clim. 4, A26 DOI: 10.1051, 2014.

Friedberg, W., Copeland, K., Duke, F. E., O'Brien III, K., & Darden Jr, E. B. Guidelines and technical information provided by the US Federal Aviation Administration to promote radiation safety for air carrier crew members. Radiation Protection Dosimetry, 86(4), 323-327, 1999.

Harrison, R. G., Nicoll, K. A., Lomas A. G., Programmable data acquisition system for research measurements from meteorological radiosondes, Rev. Sci. Instrum., 83, 036106, 2012.

Harrison, R. G., Nicoll, K. A., Lomas A. G., Geiger tube coincidence counter for lower atmosphere radiosonde measurements, Rev. Sci. Instrum., 84, 076103, 2013.

Harrison, R. G., Nicoll, K. A., Aplin, K. L., Vertical profile measurements of lower troposphere ionization. Journal of Atmospheric and Solar-Terrestrial Physics, 119, 203-210., 2014.

Hess V. F., Über beobachtungen der durchdringenden Strahlung bei sieben Freiballonfahrten, Zeitschrift fur Physik, vol. 13, pp. 1084–1091, 1912.

Israël, H. Atmospheric electricity: Atmosphärische Elektrizität. Vol. 29. Israel Program for Scientific Translations [available from the US Dept. of Commerce, National Technical Information Service, Springfield, Va.(Jerusalem), 1970.

Makhmutov, V., Bazilevskaya, G., Stozhkov, Y., Philippov, M., Yair, Y., Yaniv, R., Harrison G., Nicoll K. and Aplin, K. Cosmic ray measurements in the atmosphere at several latitudes in October, 2014, Proceeding of Science, ICRC 2015.

Mishev, Alexander, and Ilya Usoskin, Numerical model for computation of effective and ambient dose equivalent at flight altitudes-Application for dose assessment during GLEs, Journal of Space Weather and Space Climate 5, 2015.

Mironova, I. A., Aplin, K. L., Arnold, F., Bazilevskaya, G. A., Harrison, R. G., Krivolutsky, A. A., Nicoll K. A., Rozanov E. V., Turunen E. & Usoskin, I. G., Energetic Particle Influence on the Earth’s Atmosphere. Space Science Reviews, 194(1-4), 1-96, 2015.

Nicoll, K. A. "Measurements of atmospheric electricity aloft." Surveys in geophysics 33.5, 991-1057, 2012.

Nicoll, K. A., Harrison, R. G., Detection of lower tropospheric responses to solar energetic particles at midlatitudes. Physical review letters, 112(22), 225001, 2014.

Nymmik R.A., Panasyuk M.I. et Suslov A.A., Adv. Space Research, 17, (2)19-(2)30, 1996.

Pfotzer, G., Dreifachkoinzidenzen der Ultrastrahlung aus vertikaler Richtung in der Stratosphare, II, Analyse der gemessenen Kurve, Z. Phys., 102, 41–58, 1936b.

Price, C., and A. Melnikov, Diurnal, Seasonal and Inter-annual Variations in the Schumann Resonance Parameters, Journal of Atmospheric and Solar-Terrestrial Physics, 66, 1179-1185, 2004.

Regener, E.: New Results in Cosmic Ray Measurements, Nature, 132, 696–698, 1933.

Smart, D.F., M.A. Shea, A.J. Tylka, P.R. Boberg, A geomagnetic cutoff rigidity interpolation tool: Accuracy verification and application to space weather. Adv. Space Res. 37, 1206–1217, 2006.

Usoskin, I.G., K. Alanko-Huotari, G.A. Kovaltsov, K. Mursula, Heliospheric modulation of cosmic rays: Monthly reconstruction for 1951-2004, J. Geophys. Res., 110(A12), CiteID A12108, 2005.

Usoskin I., Kovaltsov G., Cosmic ray induced ionization in the atmosphere: Full modeling and practical applications, Journal of geophysical research 11, D21206, 2006.

Usoskin, I. G., G. A. Kovaltsov, and I. A. Mironova, Cosmic ray induced ionization model CRAC:CRII: An extension to the upper atmosphere, J. Geophys. Res., 115, D10302, 2010.

Yaniv, R., Yair, Y., Price, C., & Katz, S., Local and global impacts on the fair-weather electric field in Israel. Atmospheric Research, Vol 172-173, p. 119-125, 2016.

Figure Captions:

Figure 1. Ionization-altitude curves of ionization from cosmic radiation. (left) past rocket launch [adapted from Israël 1970 his figure 26] and (right) modern balloon launch. [adapted from Harrison et al 2014]

Figure 2. Regional map of Israel and surrounding countries with flight trajectories for each launch.

Figure 3. Vertical temperature profile (a), pressure profile (b) and relative humidity profile (c) for each launch. We note the locations of several cloud types, based on the RH values and visual observations.

Figure 4. Ionization variation versus the altitude [km] (a) and Vertical Ionization profile [counts mins^{-1}, cpm] versus the Pressure [mbar] (b). The black line shows the average value of 6 launches

Figure 5. Modulation potential as a function of the Ionization count rate shows the effect of Solar cycle 24 phase on the Ionization in low latitudes.

Figure 6. Ionization curves from Mitzpe Ramon (Israel), Zaragoza-Barcelona (Spain) and Reading (UK).

Figure 7. Model results of Ion production rate versus altitude from Mitzpe Ramon (Israel), -Barcelona (Spain) and Reading (UK) of the 14 May 2015 Balloon launch.

Figure 8. Observations and modelled ion production rates (top) 14 May 2015 flight and (bottom) 22 Oct 2014 flight.

Table Captions

Table 1. Summary of balloon launches. (*) Ascent only.

Launch	Date	Modulation potential [MV]	Flight Duration [s]	Peak Altitude [m]	Pressure [mbar] at peak	Lowest Temperature [°C] recorded	(RP max) cpm @ [km]
1*	6 Oct 2014	677	3149	17542	85.5	-72.3 @ 16.3 km	28.1 cpm at 16.2 km
2*	22 Oct 2014	621	5342	29467	12.6	-74.7 @ 17.2 km	36.1 cpm at 18.5 km
3	14 May 2015	656	6325	28320	15.2	-63.9 @ 20.2 km	31.3 cpm at 16.07 km
4	27 Aug 2015	573	9351	34796	6.1	-74 @ 16.7 km	40.80 cpm at 21.8 km
5*	20 Jun 2016	449	6431	35496	5.4	-74.5 @ 17.5 km	50.87 cpm at 17.1 km
6*	30 Aug 2016	337	7639	28200	16.67	-80.7 @ 17.6 km	47.1 cpm at 19 km

Figures:

Figure 1:

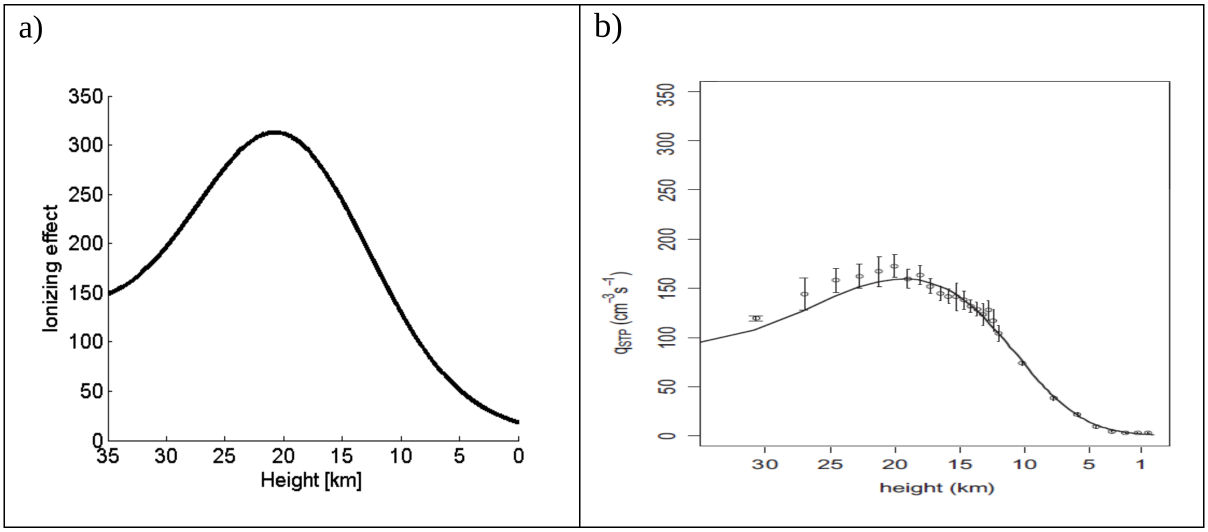

Figure 2:

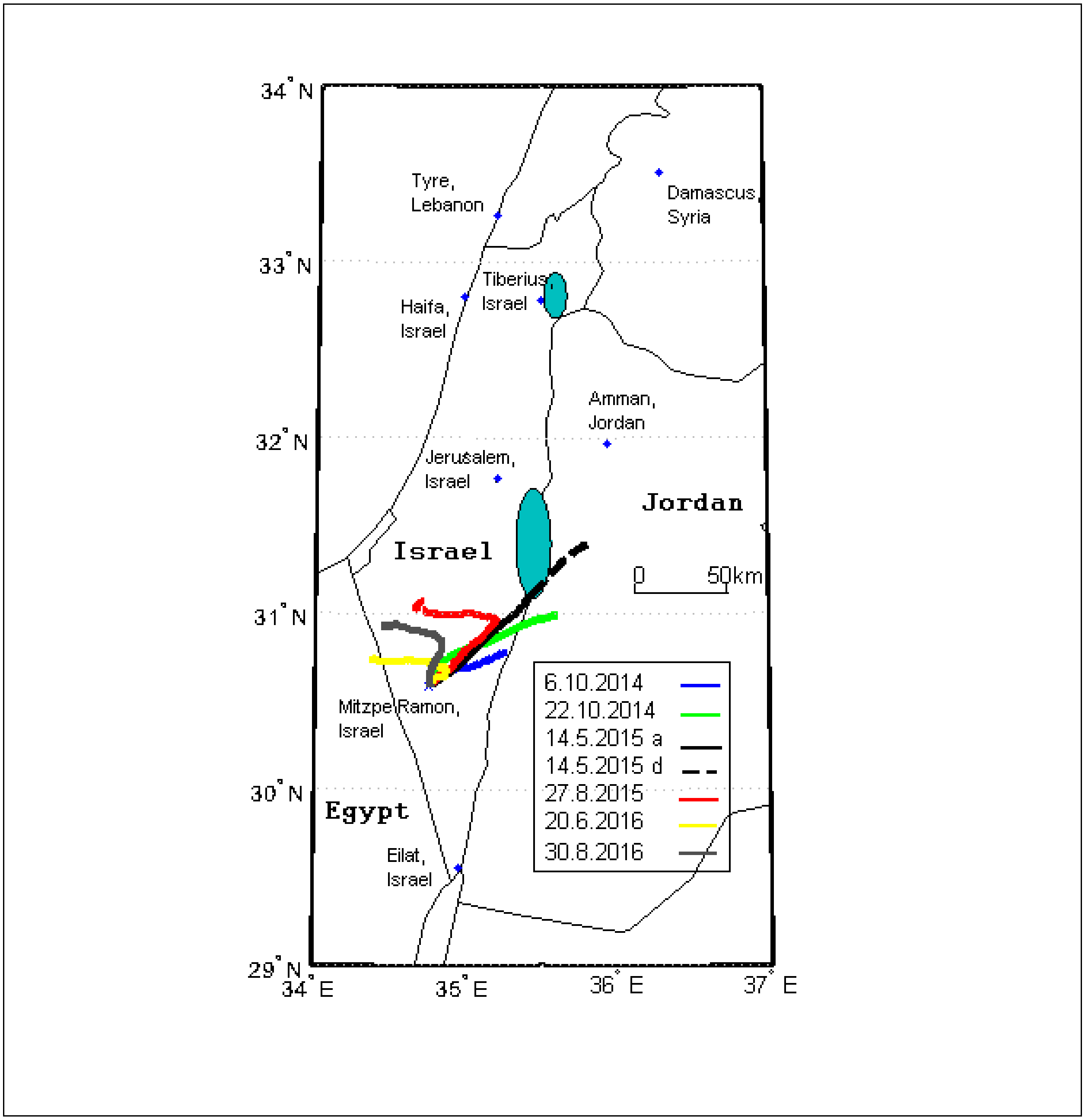
34° N
33° N
32° N
31° N
30° N
29° N
34° E
35° E
36° E
37° E
Tyre, Lebanon
Damascus, Syria
Haifa, Israel
Tiberius, Israel
Amman, Jordan
Jerusalem, Israel
Jordan
Israel
0 50km
Mitzpe Ramon, Israel
Egypt
Eilat, Israel
6.10.2014
22.10.2014
14.5.2015 a
14.5.2015 d
27.8.2015
20.6.2016
30.8.2016

368 **Figure 3:**

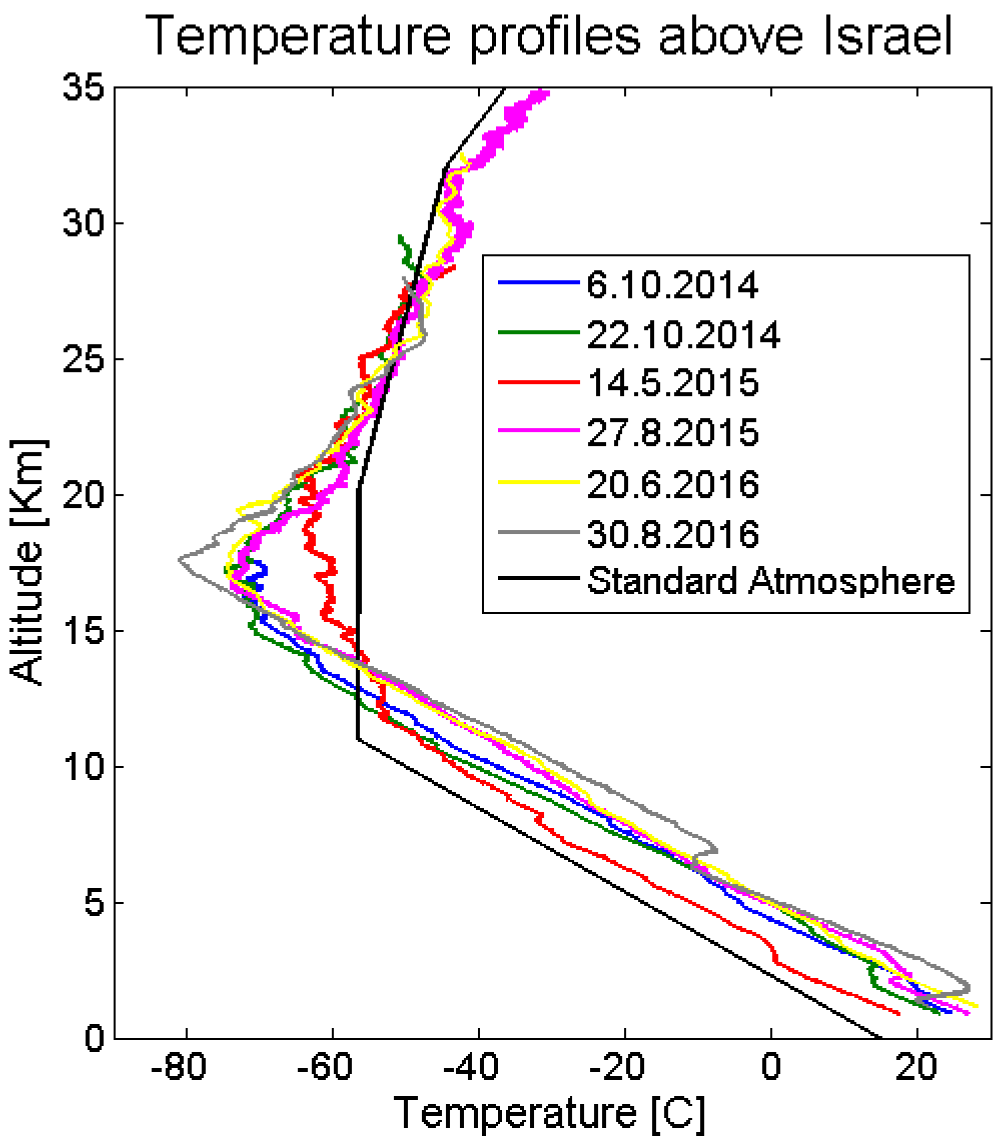

a)

b)

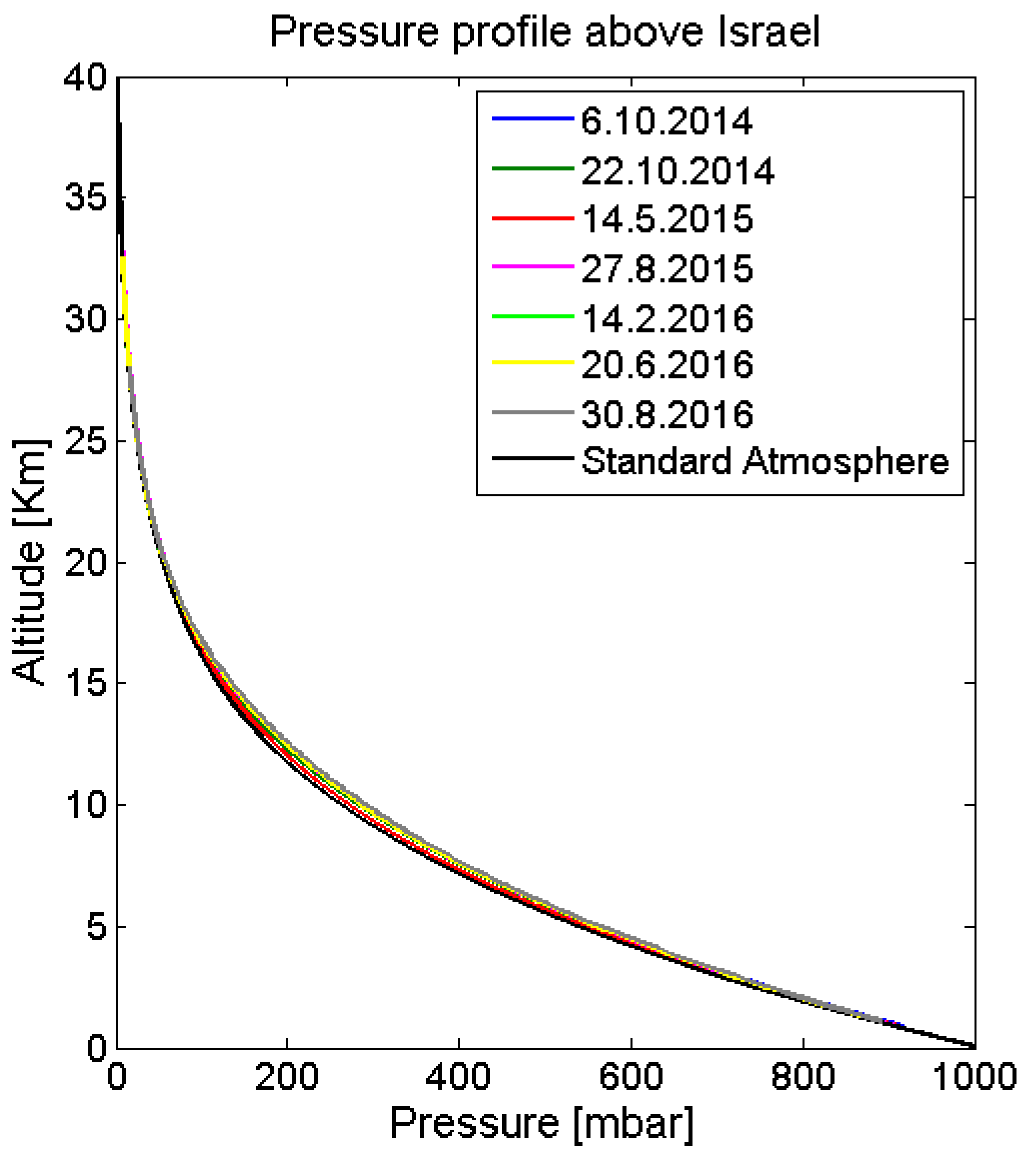

Pressure profile above Israel
40
35
30
25
20
15
10
5
0
Altitude [Km]
0
200
400
600
800
1000
Pressure [mbar]
6.10.2014
22.10.2014
14.5.2015
27.8.2015
14.2.2016
20.6.2016
30.8.2016
Standard Atmosphere

c)

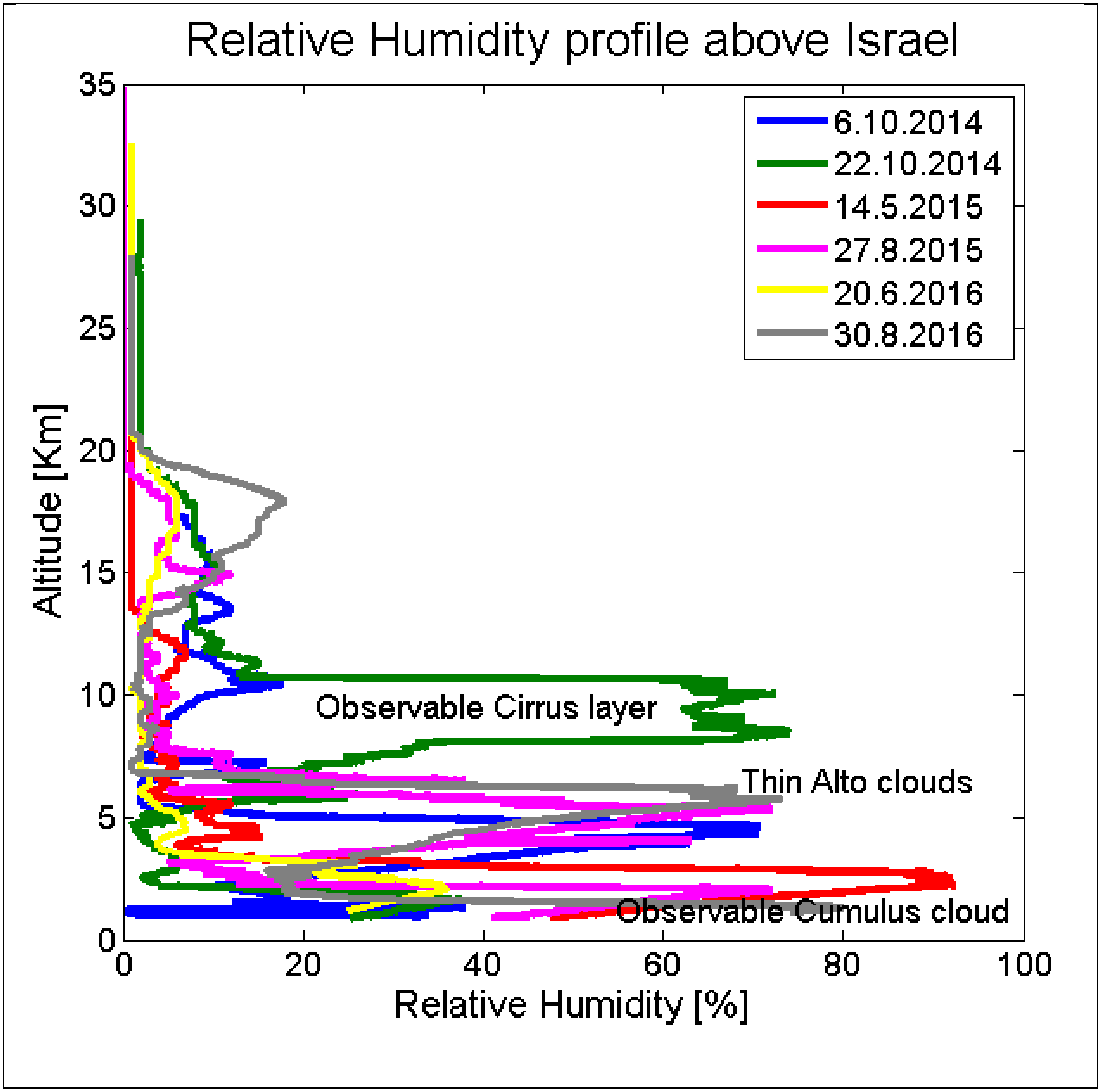
Relative Humidity profile above Israel
Altitude [Km]
Relative Humidity [%]
6.10.2014
22.10.2014
14.5.2015
27.8.2015
20.6.2016
30.8.2016
Observable Cirrus layer
Thin Alto clouds
Observable Cumulus cloud
0
5
10
15
20
25
30
35
0
20
40
60
80
100

Figure 4:

a)

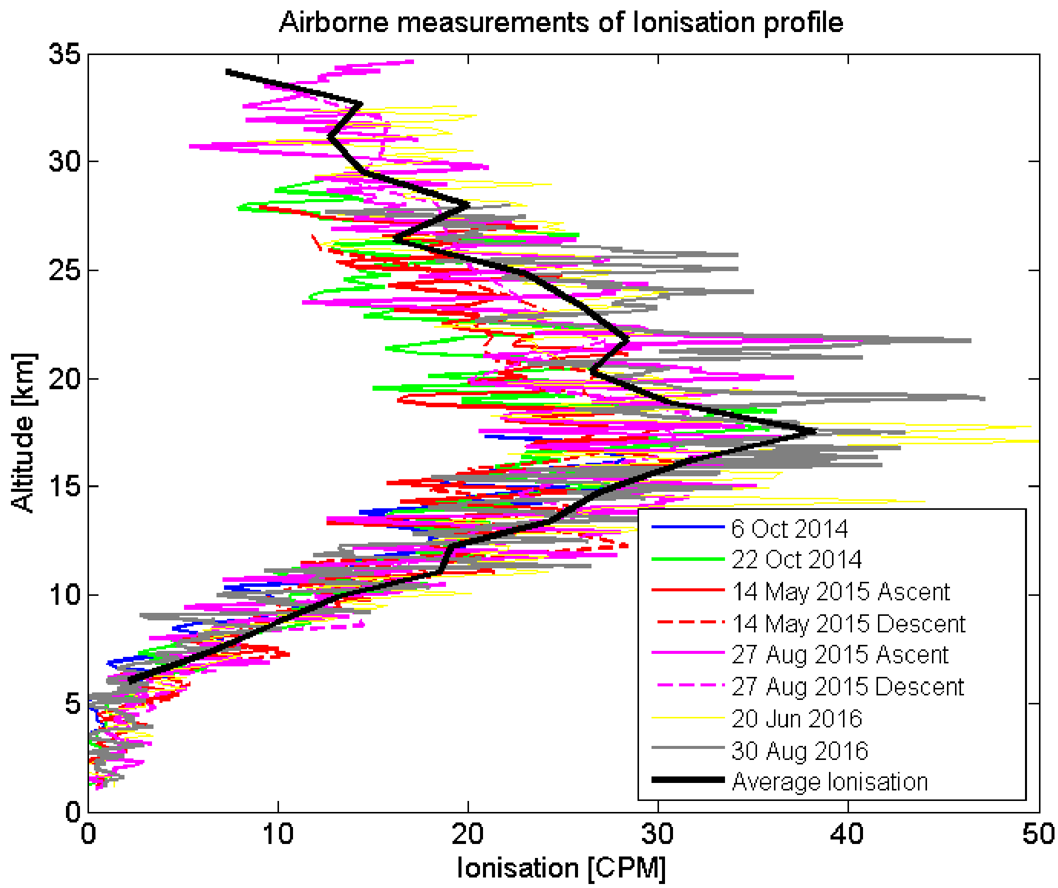

Airborne measurements of Ionisation profile
Altitude [km]
Ionisation [CPM]
0
5
10
15
20
25
30
35
0
10
20
30
40
50
6 Oct 2014
22 Oct 2014
14 May 2015 Ascent
14 May 2015 Descent
27 Aug 2015 Ascent
27 Aug 2015 Descent
20 Jun 2016
30 Aug 2016
Average Ionisation

b)

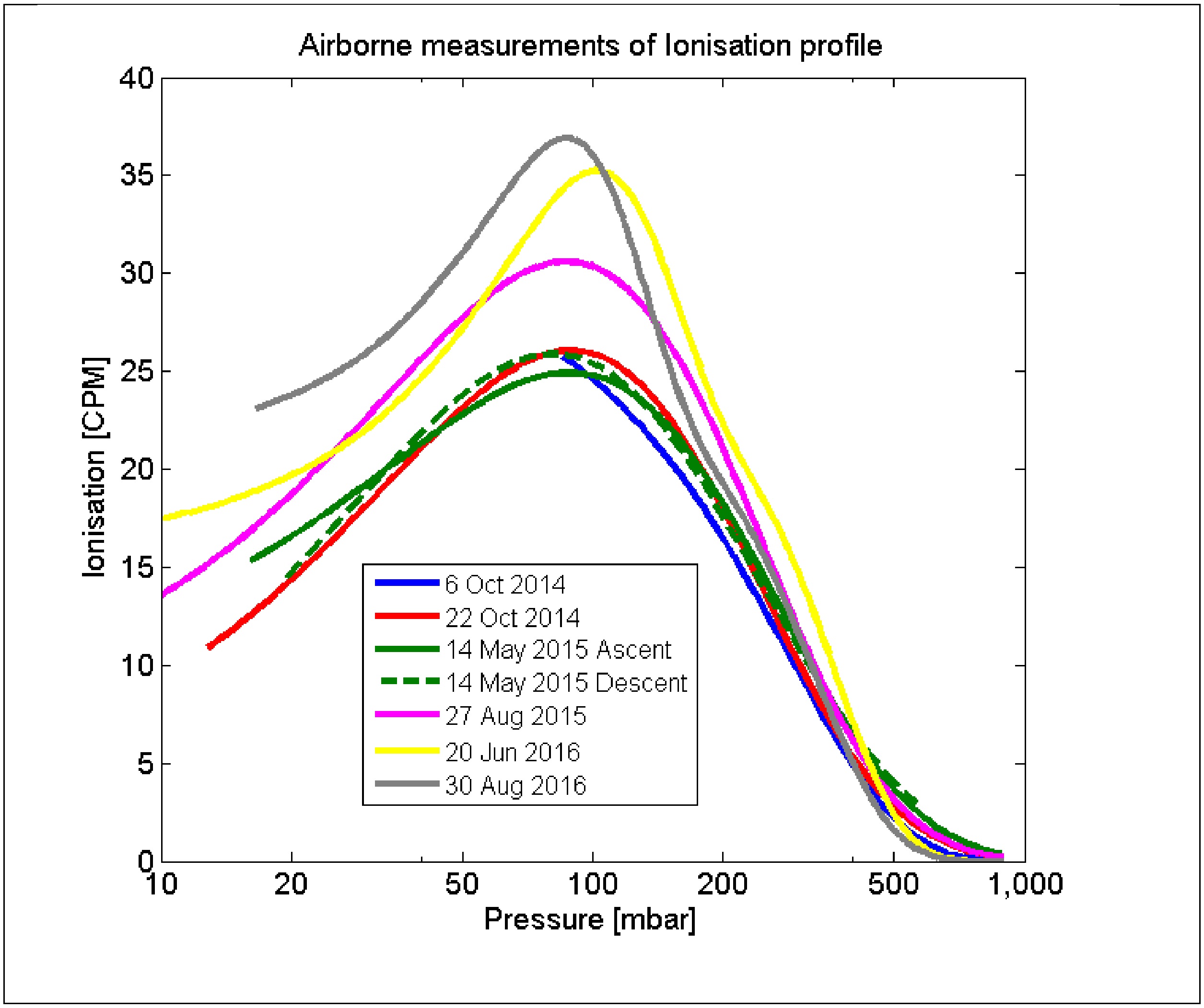
Airborne measurements of Ionisation profile
Ionisation [CPM]
0
5
10
15
20
25
30
35
40
10
20
50
100
200
500
1,000
Pressure [mbar]
6 Oct 2014
22 Oct 2014
14 May 2015 Ascent
14 May 2015 Descent
27 Aug 2015
20 Jun 2016
30 Aug 2016

Figure 5:

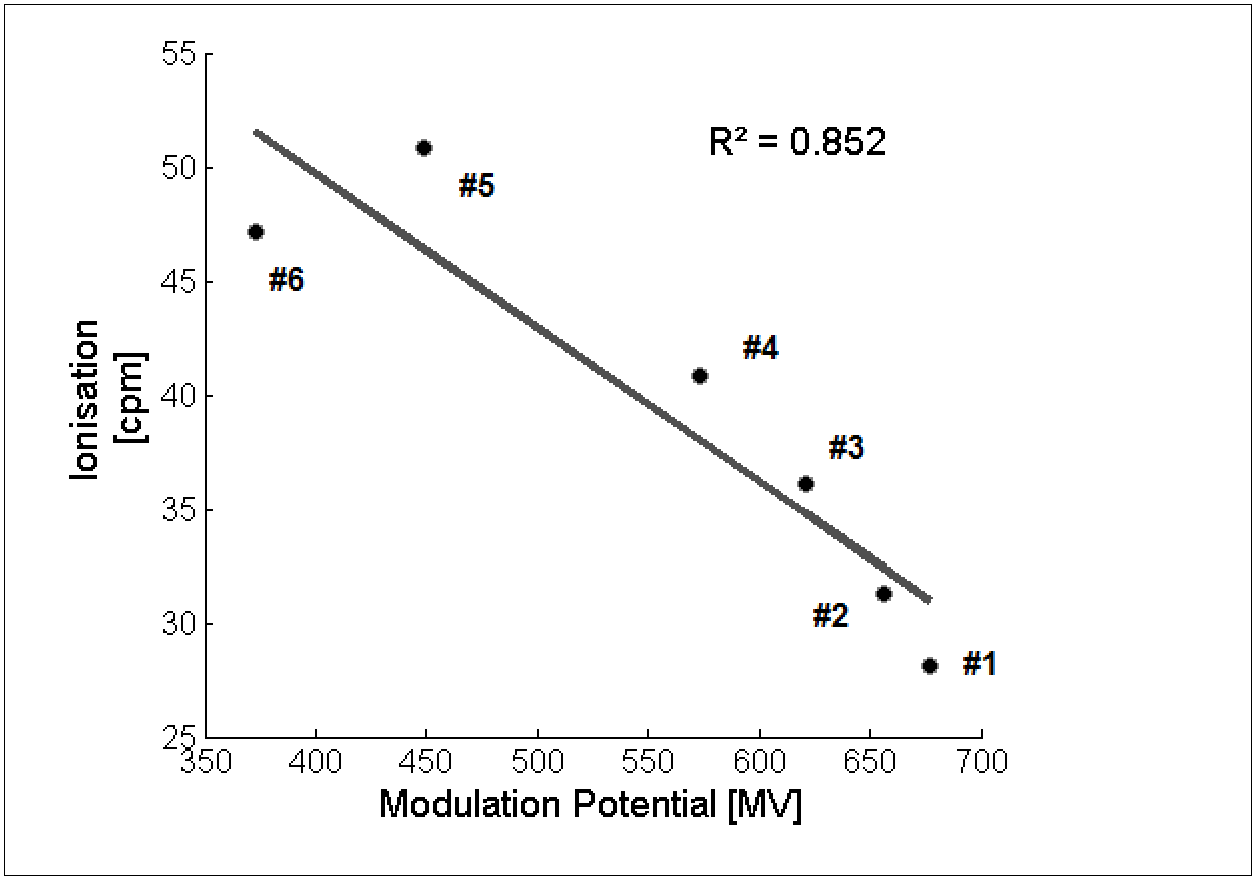
R² = 0.852
#5
#6
#4
#3
#2
#1
Ionisation [cpm]
Modulation Potential [MV]
55
50
45
40
35
30
25
350
400
450
500
550
600
650
700

Figure 6:

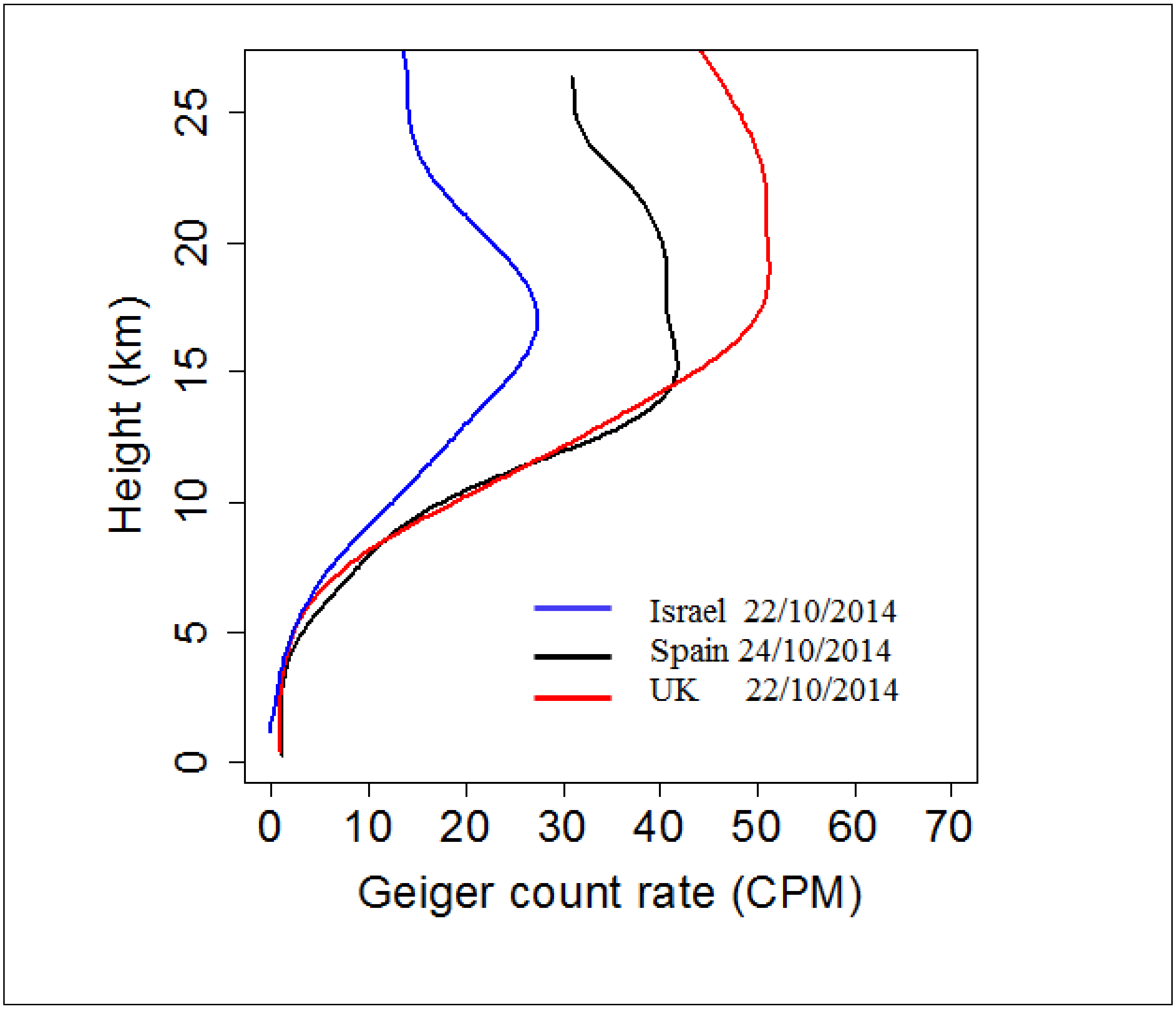
Height (km)
0
5
10
15
20
25
0
10
20
30
40
50
60
70
Geiger count rate (CPM)
Israel 22/10/2014
Spain 24/10/2014
UK 22/10/2014

Figure 7:

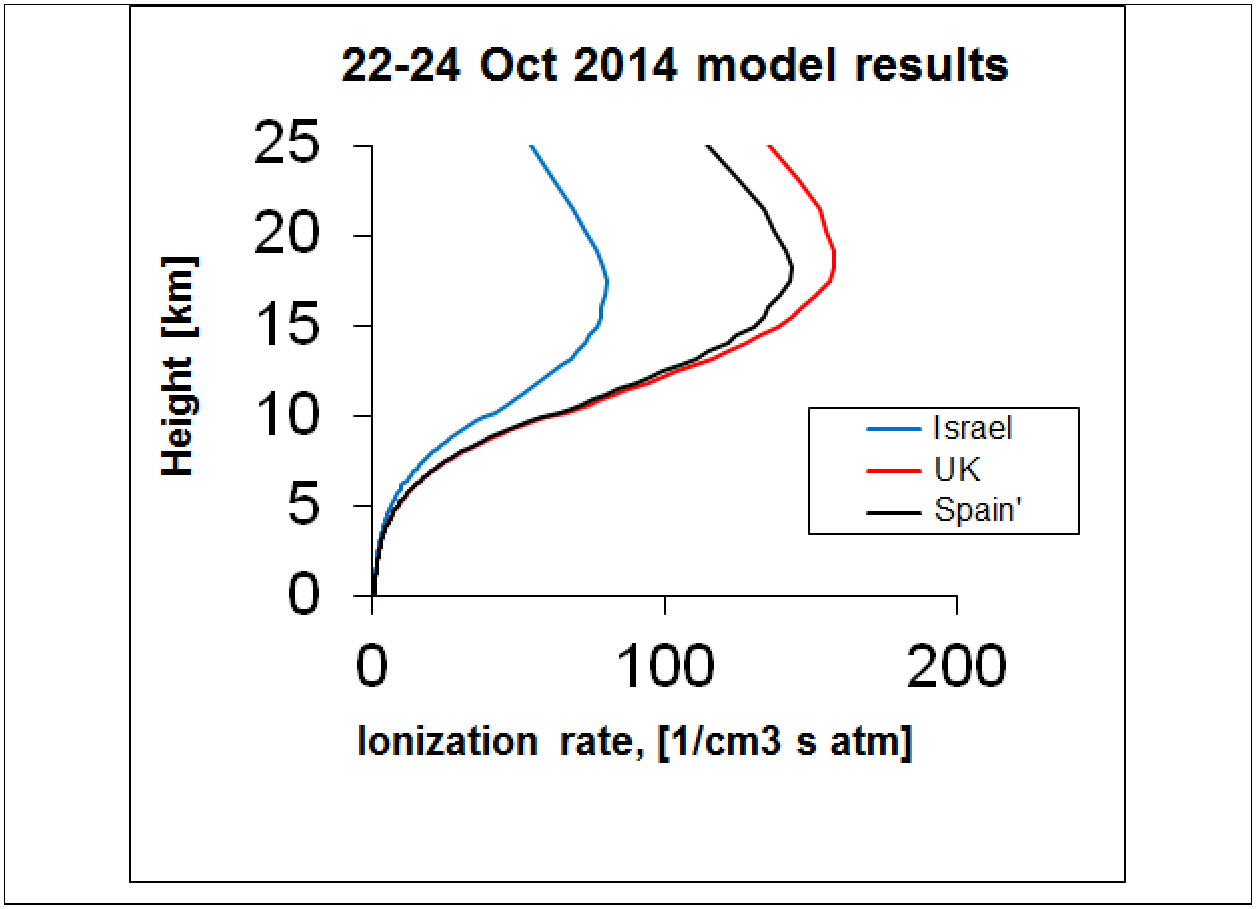

Figure 8:

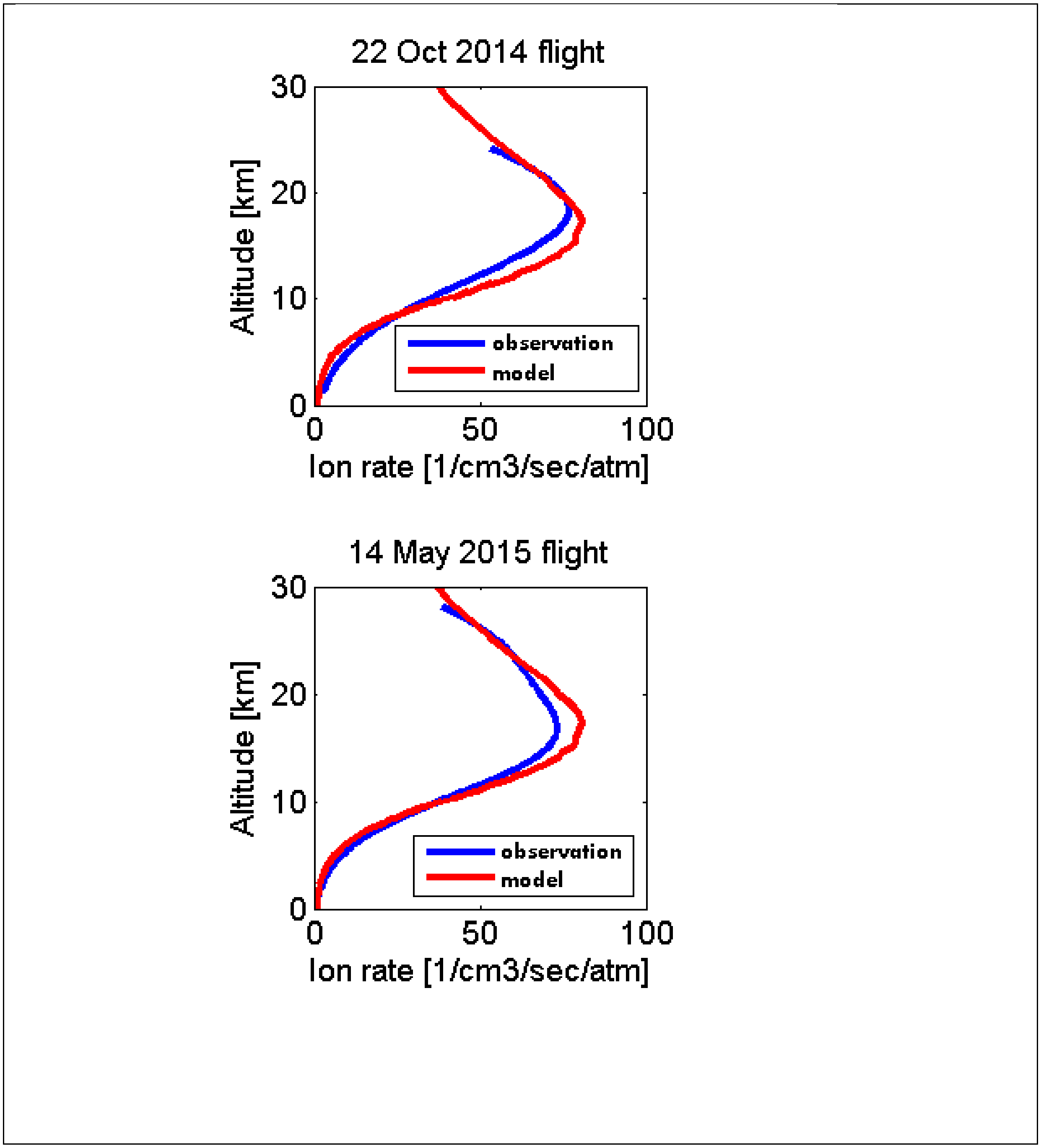
22 Oct 2014 flight
Altitude [km]
Ion rate [1/cm3/sec/atm]
observation
model
0
10
20
30
0
50
100
14 May 2015 flight
Altitude [km]
Ion rate [1/cm3/sec/atm]
observation
model
0
10
20
30
0
50
100